

Emergence of noncollinear magnetic ordering in small magnetic clusters: Mn_n and As@Mn_n clusters

Mukul Kabir,^{1,2,*} D. G. Kanhere³ and Abhijit Mookerjee¹

¹*Department of Materials Science, S.N. Bose National Center for Basic Sciences, JD Block, Sector III, Salt Lake City, Kolkata 700 098, India.*

²*Department of Materials Science and Engineering, Massachusetts Institute of Technology, Cambridge, Massachusetts 02139, USA.*

³*Department of Physics and Center for Modeling and Simulation, University of Pune, Pune - 411 007, India.*

(Dated: February 1, 2008)

Using first-principles density functional calculations, we have studied the magnetic ordering in pure Mn_n ($n=2-10, 13, 15, 19$) and As@Mn_n ($n=1-10$) clusters. Although, for both pure and doped manganese clusters, there exists many collinear and noncollinear isomers close in energy, the smaller clusters with $n \leq 5$ have collinear magnetic ground state and the emergence of noncollinear ground states is seen for $n \geq 6$ clusters. Due to strong $p-d$ hybridization in As@Mn_n clusters, the binding energy is substantially enhanced and the magnetic moment is reduced compared to the corresponding pure Mn_n clusters.

PACS numbers: 75.75.+a, 36.40.Cg, 61.46.Bc, 73.22.-f

I. INTRODUCTION

Noncollinear magnetism, i.e. magnetic ordering where the local magnetic moments are not parallel or antiparallel to a global direction, exists in a variety of systems, for example, in topologically frustrated antiferromagnets, in spiral spin-density waves and spin-spiral states. These types of orderings can be called interatomic noncollinear magnetism since the different atomic moments are noncollinear. Generally, noncollinear configurations occur more easily in a low symmetry or a disordered magnetic system.^{1,2} Thus small clusters, which have less symmetry constraints than the bulk, are likely candidates for noncollinear structures. Indeed, as a consequence of spin-spiral ground state of fcc Fe (Refs. 3 and 4) and spin density wave ground state of bcc Cr (Ref. 5), the small Fe_n and Cr_n clusters were found to have noncollinear magnetic structures.^{6,7,8,9,10}

From the structural and magnetic point of view, manganese is one of the most complex of all metals and has attracted considerable attention. The electronic configuration in a Mn atom is $4s^2 3d^5$ and consequently Mn atoms have high magnetic moments of $5 \mu_B$. High $4s^2 3d^5 \rightarrow 4s^1 3d^6$ promotion energy means that Mn atoms do not bind strongly when they are brought together to form a cluster or a bulk solid. The most stable polymorph, α -Mn, has an exotic crystal structure containing 58 atoms in a cubic unit cell. This α -Mn exhibits a complex antiferromagnetic order below the Néel temperature of 95 K and is nonmagnetic at room temperature.¹¹ The magnetic transition of α -Mn is coupled to a tetragonal distortion. Recent density functional calculations indicate a noncollinear magnetic ground state for α -Mn.¹² The other polymorph of Mn, known as β -Mn, also has a stable noncollinear configuration even though the ground state is weakly ferrimagnetic.¹³ These results are in good agreement with the neutron scattering,¹⁴ magnetic torque¹⁵ and nuclear magnetic resonance¹⁶ experi-

ments, where the experimental results are interpreted in terms of noncollinear antiferromagnetic structure.

As mentioned earlier small Mn clusters, which have less symmetry constraints, are likely candidates for the occurrence of noncollinear magnetic structure. However, majority of the theoretical calculations have been made under the collinear spin assumption.^{17,18,19,20,21} Among them, most extensive study has been done by Kabir *et al.*, where the structural and magnetic properties of Mn_n clusters in the size range $n=2-20$ have been investigated using density functional theory.²¹ It was found that Mn_2 , Mn_3 and Mn_4 exhibit ferromagnetic ordering, whereas a magnetic transition to the ferrimagnetic ordering takes place at $n=5$ and the ferrimagnetic state continues to be the ground state for clusters with $n > 5$. The predicted magnetic moments are in well agreement with the Stern-Gerlach (SG) clusters beam experiments.^{22,23} However very recently,²⁴ we pointed out that the noncollinear treatment of spins is indeed necessary at the size range $n \geq 6$. Morisato *et al.* studied Mn_5 and Mn_6 clusters and found Mn_6 to be the smallest cluster to exhibit noncollinear ground state.²⁵ However, using local spin density approximation Longo *et al.* found that all the clusters in the size range $n=3-7$ have noncollinear ground states.²⁶ Recently, noncollinear magnetic ordering has also been found in small Mn-clusters supported on a Cu(111) surface.²⁷ In this study however, the cluster geometries have been assumed planar and they were placed on a regular face centered-cubic Cu lattice with experimental lattice parameters. No structural relaxation for either the surface or the cluster was considered.

The present paper is the sequel of our earlier reports.^{21,24} In this paper, we allow noncollinear ordering of atomic moments and extensively study how collinear and noncollinear magnetic ordering evolves in small Mn_n clusters and how the magnetic ordering gets perturbed if we dope a single nonmagnetic atom (for example an As-atom) into it. This

is important as (III,Mn)V semiconductors show ferromagnetism and the effect of Mn-clustering is being debated for a long time.^{24,28,29,30,31,32,33} Moreover, the noncollinear ferromagnetism is common in (III,Mn)V semiconductors.^{34,35,36,37,38} Experimental study by Potashnik *et al.*^{34,35} indicated that the Curie temperature, the ground state saturation magnetization $M(T = 0)$ and the shape of the $M(T)$ curve all depend upon the temperature and annealing. These can be explained only if the noncollinearity in the localized Mn magnetic moments is considered in the ground state.^{36,37,38} From this point of view, it will be very interesting to investigate whether small As@Mn_n clusters do show noncollinearity or not.

II. METHOD

In the theoretical approaches to noncollinear magnetism,^{39,40,41,42} the wave functions are described by two-component spinors, $\Psi(\mathbf{r}) \equiv (\Psi^\alpha(\mathbf{r}), \Psi^\beta(\mathbf{r}))$, where α and β are the spin indices. The density matrix is defined as,

$$\rho_{\alpha\beta} = \sum_i f_i \Psi_i^\alpha(\mathbf{r}) \Psi_i^{\beta*}(\mathbf{r}), \quad (1)$$

where f_i is the occupation number of the single-particle state.

The charge $n(\mathbf{r})$ and magnetization $\vec{m}(\mathbf{r})$ parts of the density matrix can be extracted by expanding in terms of the Pauli spin matrices σ_k ($k = x, y, z$),

$$\rho(\mathbf{r}) = \frac{1}{2} \left[n(\mathbf{r})\mathbf{1} + \sum_k m_k(\mathbf{r})\sigma_k \right], \quad (2)$$

where m_k is the Cartesian components of $\vec{m}(\mathbf{r})$. The exchange-correlation potential, $v_{xc} = v_0(\mathbf{r})\mathbf{1} + \vec{\xi}(\mathbf{r}) \cdot \vec{\sigma}$, contains nonmagnetic and magnetic parts. The nonmagnetic part v_0 and $|\vec{\xi}|$ are given as a function of n and $|\vec{m}|$ in the same way that is done in the case of collinear magnetism, but here in addition $\vec{\xi}(\mathbf{r})$ is always parallel to $\vec{m}(\mathbf{r})$. In this scheme, the individual eigenstates can have different spin quantization directions and furthermore, the spin quantization axis of the each state can vary with position.

Calculations have been performed using density functional theory (DFT) within the pseudopotential plane wave method. The projector augmented wave method⁴³ has been used and for the spin-polarized gradient approximation to the exchange-correlation energy we used the Perdew-Burke-Ernzerhof functional,⁴⁴ as implemented in the Vienna *ab-initio* Simulation Package.⁴⁵ The 3*d*, 4*s* for Mn and 4*s*, 4*p* orbitals for As are treated as valence states. The spinor wave functions are expanded in a plane wave basis set with the kinetic energy cutoff 337.3 eV. We have ensured that the cutoff is sufficient by varying it up to 600 eV and found that the energy

difference between ferromagnetic and antiferromagnetic states converges within ~ 1 meV for Mn₂ and As@Mn₂. Calculations have been carried out at the Γ -point. We adopted periodic boundary conditions and described the cluster within a large simple cubic supercell such that the periodic images are separated by at least 12 Å of vacuum. This essentially ensures negligible interactions between the periodic images. Symmetry unrestricted optimizations were performed using quasi-Newtonian and conjugate gradient methods until all the force components become less than 0.005 eV/Å. For a particular sized Mn_n and As@Mn_n cluster, several different initial structures were studied to ensure that the globally optimized geometry does not correspond to a local minima, and to be extensive, both noncollinear and collinear magnetic structures have been considered separately. Moreover, we explicitly considered all possible spin multiplicities for the collinear case.

For a collinear spin cluster all the spins are parallel (0°) or antiparallel (180°) to each other. On the other hand, the angle between any two moments could be anything in between 0° and 180° for a noncollinear case and the deviation from 0° or 180° is termed ‘‘degree of noncollinearity’’. The average degree of noncollinearity for a particular cluster can be defined as,

$$\theta = \frac{\sum_{i,<j} |\Theta - \theta_{ij}|}{\sum_k^{N-1} (N - k)}, \quad (3)$$

where ij runs for all independent spin pairs and $\sum_k^{N-1} (N - k)$ is the total number of such independent spin(atom) pairs with N being the number of atoms in the cluster. Θ is either 0° or 180° and θ_{ij} is the angle between i -th and j -th moment.

III. RESULTS AND DISCUSSION

A. Pure Mn_n clusters: Collinear vs noncollinear ordering

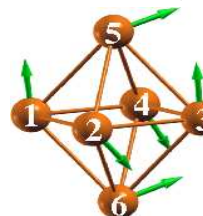
In an earlier work, we have studied the magnetic ordering of pure Mn_n ($n \leq 20$) clusters within the collinear atomic moment assumption.²¹ Above a certain cluster size ($n=5$), the magnetic ordering is found to be ferrimagnetic and the calculated magnetic moments were in good agreement²¹ with Stern-Gerlach experiments.^{22,23} However, the validity of the collinear spin assumption should be checked rigorously because, in principle, the complex ferrimagnetic ordering and magnetic ‘frustration’⁴⁶ could definitely lead to the noncollinear ordering in magnetic clusters. The type of magnetic ordering along with the total magnetic moment and relative energy difference with the ground state are given in the Table I and the optimal noncollinear structures are shown in Fig.1 ($n=3-10$) and Fig.2 ($n=13, 15$ and 19) for pure Mn_n clusters.

TABLE I: Type of magnetic ordering, average degree of non-collinearity (θ), total magnetic moment (M_{tot}) and the relative energy difference ($\Delta E = E - E_{\text{GS}}$) for pure Mn_n clusters for $n=2-10, 13, 15$ and 19 .

| Cluster | Magnetism | θ ($^\circ$) | M_{tot} (μ_B) | ΔE (meV) |
|------------------|--------------|--------------------------|---------------------------------|---------------------|
| Mn_2 | collinear | - | 10 | 0 |
| Mn_3 | collinear | - | 15 | 0 |
| | noncollinear | 42 | 8.54 | 35 |
| | noncollinear | 38.89 | 8.27 | 36 |
| | noncollinear | 44 | 8.77 | 38 |
| | collinear | - | 5 | 46 |
| | noncollinear | 55.5 | 3.63 | 325 |
| Mn_4 | collinear | - | 20 | 0 |
| | noncollinear | 4.98 | 19.96 | 31 |
| | collinear | - | 10 | 78 |
| Mn_5 | collinear | - | 3 | 0 |
| | noncollinear | 12.05 | 4.43 | 18 |
| | noncollinear | 51.94 | 12.46 | 60 |
| | collinear | - | 13 | 60 |
| | collinear | - | 5 | 79 |
| Mn_6 | noncollinear | 48.8 | 12.83 | 0 |
| | noncollinear | 9.26 | 8.48 | 96 |
| | collinear | - | 8 | 123 |
| | collinear | - | 2 | 140 |
| Mn_7 | collinear | - | 5 | 0 |
| | collinear | - | 7 | 91 |
| | collinear | - | 3 | 192 |
| | noncollinear | 0.63 | 5.00 | 232 |
| | noncollinear | 48.12 | 2.86 | 241 |
| Mn_8 | noncollinear | 22.85 | 6.83 | 0 |
| | collinear | - | 8 | 170 |
| | collinear | - | 12 | 170 |
| | collinear | - | 10 | 200 |
| Mn_9 | noncollinear | 48 | 5.33 | 0 |
| | noncollinear | 1.92 | 0.99 | 50 |
| | noncollinear | 39.88 | 5.62 | 133 |
| | collinear | - | 7 | 181 |
| Mn_{10} | noncollinear | 42 | 5.04 | 0 |
| | noncollinear | 43.95 | 3.30 | 24 |
| | collinear | - | 14 | 81 |
| Mn_{13} | noncollinear | 2.56 | 3.15 | 0 |
| | collinear | - | 3 | 0 |
| | noncollinear | 6.85 | 3.80 | 11 |
| | collinear | - | 7 | 77 |
| | noncollinear | 5.06 | 3.37 | 269 |
| | noncollinear | 30.37 | 11.57 | 304 |
| Mn_{15} | collinear | - | 13 | 0 |
| | noncollinear | 0.90 | 13.00 | 26 |
| | collinear | - | 5 | 33 |
| | noncollinear | 4.70 | 12.91 | 49 |
| | noncollinear | 8.03 | 26.85 | 343 |
| Mn_{19} | collinear | - | 21 | 0 |
| | noncollinear | 4.55 | 20.89 | 5 |
| | collinear | - | 19 | 9 |
| | collinear | - | 9 | 74 |

The case of triangular Mn_3 is very interesting. If the triangle is equilateral and the magnetic ordering is anti-

TABLE II: Magnetic moments (μ_B) and angles (θ_{ij} in degree) between the moments for the noncollinear ground state of Mn_6 with $12.83 \mu_B$ magnetic moment.



| i/j | 1 | 2 | 3 | 4 | 5 | 6 | Moment |
|-------|-----|-----|-----|-----|----|----|--------|
| 1 | - | 156 | 2 | 146 | 77 | 75 | 3.62 |
| 2 | 156 | - | 154 | 9 | 79 | 80 | 3.64 |
| 3 | 2 | 154 | - | 145 | 75 | 74 | 3.62 |
| 4 | 146 | 9 | 145 | - | 70 | 71 | 3.63 |
| 5 | 77 | 79 | 75 | 70 | - | 1 | 3.80 |
| 6 | 75 | 80 | 74 | 71 | 1 | - | 3.80 |

ferromagnetic then the third atom doesn't know how to align and, consequently, is in the 'frustrated' state. This frustration could either be removed by reducing its geometrical symmetry or by adopting noncollinear magnetic order or both. The ground state is collinear ferromagnetic with $5 \mu_B$ /atom magnetic moment and has equilateral triangular geometry. The optimal noncollinear structure is found to be the next isomer, which lies 35 meV higher in energy. This structure has high noncollinearity and has a total magnetic moment of $8.54 \mu_B$ (Fig.1a). The geometrical structure for this state is a isosceles triangle. We also find several noncollinear (Fig.1b-d) and collinear (Table I) magnetic states which lie close in energy. However, triangular Mn_3 cluster prefers noncollinear structure when it is placed on a Cu(111) surface, and each moment lie parallel to the Cu(111) surface and make an equal angle of 120° to its neighbor.²⁷ For this case, it has also been pointed out that the intra cluster exchange parameter is much stronger than that of inter cluster, which means that the magnetic ordering is not affected if cluster-cluster distance becomes very small.

For the Mn_4 cluster, a collinear ferromagnetic ground state with $20 \mu_B$ magnetic moment is found to be the ground state. The optimal noncollinear structure (Fig.1e) lies only 31 meV higher in energy and has comparable magnetic moment. In contrast, Longo *et al.*²⁶ found a noncollinear ground state with very small magnetic moment, $4.5 \mu_B$, to be the ground state. It has to be noted that they had used a different level of approximation (local spin density approximation (LDA)) for the exchange-correlation, which might be the reason for this discrepancy. Although there are no available report of magnetic ordering for Mn_4 in the gas phase, Ludwig *et al.*⁴⁷ observed a 21-line hyperfine pattern in solid silicon, which establishes that all the four atoms in Mn_4 are equivalent and has a total magnetic moment of $20 \mu_B$.

The Mn_5 cluster has been investigated by many authors but most of them have restricted themselves to the collinear spin assumption.^{17,18,19,21} However, few attempts have made to investigate noncollinear magnetic ordering.^{24,25,26} We find the collinear ferrimagnetic ground state (Fig.1f) lies slightly lower (18 meV) in energy than the optimal noncollinear state. The average degree of noncollinearity found for this structure is 12° . The state next higher in energy is the noncollinear structure ($12.46 \mu_B$, $\theta \sim 52^\circ$, shown in Fig.1g) and the degenerate

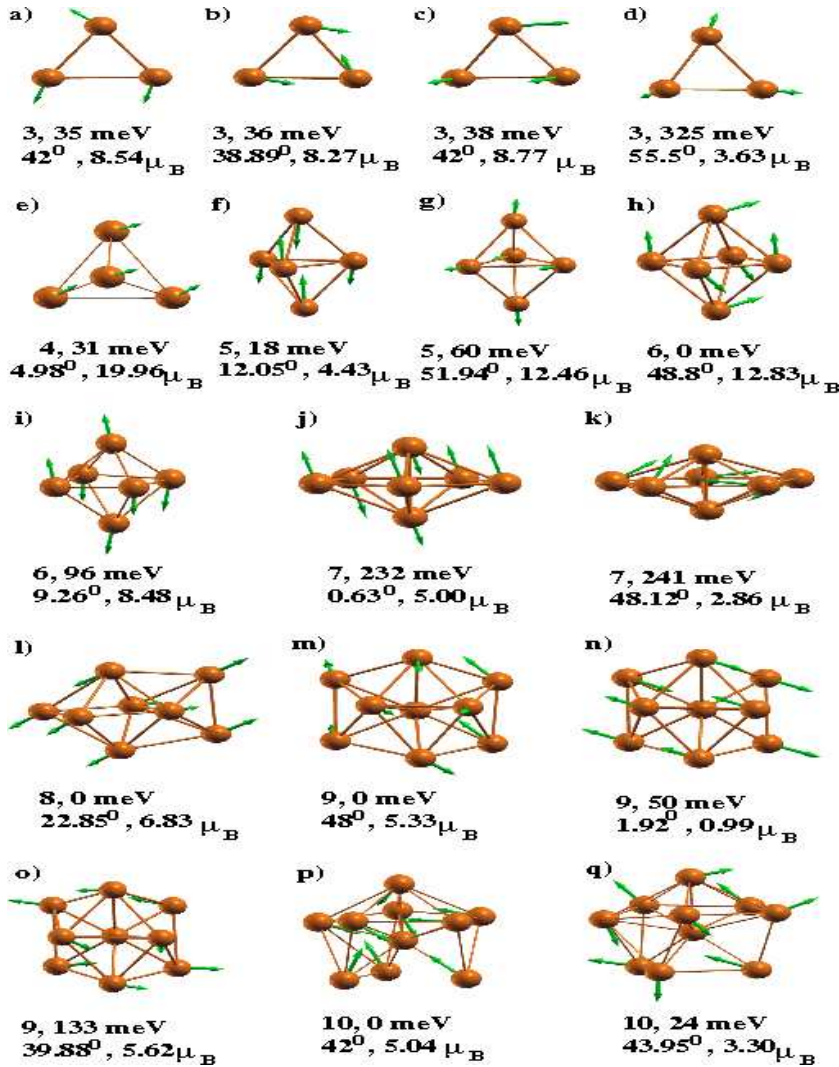


FIG. 1: (color online) Optimal non-collinear structures for Mn_n clusters in the size range $n = 3-10$. The first line gives the number of atoms n in the cluster and the energy relative to the corresponding ground state, ΔE , (meV), whereas, the second line represents the average degree of non-collinearity (θ in degree) and the corresponding total magnetic moment (μ_B). The optimal collinear structures are not shown here rather we refer to Kabir *et al.*²¹

ferrimagnetic collinear structure. These are followed by another collinear ferrimagnetic structure slightly higher in energy.²¹

The Mn_6 cluster is found to be the smallest cluster, which has noncollinear magnetic order in the ground state (Fig.1h). This magnetic structure has high non-collinearity ($\theta \sim 49^\circ$, the angles θ_{ij} between the Mn-moments are given in Table II) and its geometric structure is a distorted octahedron. The magnetic moment is $12.83 \mu_B$. Present result agrees with Morisato *et al.*,²⁵ who found a noncollinear state with $12.24 \mu_B$ moment as the ground state. The isomer next higher in energy by 96 meV is the noncollinear structure with total moment $8.48 \mu_B$. Next higher energy isomers are four collinear structures with moments 8, 2, 16 and $26 \mu_B$.²¹

The ground state for Mn_7 is collinear with a total magnetic moment of $5 \mu_B$. Next higher in energy are two collinear isomers with a total 7 and $3 \mu_B$ moments (Table I). As discussed in our previous work,²¹ this is the plausible reason for the large experimental uncertainty observed, $0.72 \pm 0.42 \mu_B/\text{atom}$.²² The optimal noncollinear structure lies much higher (232 meV) in en-

ergy and has a magnetic moment which is same as the collinear ground state (Fig.1j). However, a noncollinear state has been reported to be the ground state in an earlier report,²⁶ where the exchange-correlation energy has been approximated within LDA.

These results in the size range ($n \leq 7$) agree well with Morisato *et al.*²⁵ They have adopted same level of theory used in the present report to study Mn_5 and Mn_6 clusters and found the Mn_6 cluster to be the smallest one which shows noncollinear magnetic ordering. On the other hand, Longo *et al.*²⁶ studied Mn_3 – Mn_7 clusters within some different level of theory. They have used LDA for the exchange-correlation energy and found the magnetic ordering to be noncollinear for all the clusters in the size range $n = 3-7$.

As it has been discussed in our previous report²¹ that we have considered many different initial structures for Mn_8 cluster. However, when we allow noncollinearity among the atomic moments, we find a noncollinear bi-capped octahedral structure with magnetic moment $6.83 \mu_B$ to be the ground state (Fig.1l). The moment of the noncollinear ground state, $0.85 \mu_B/\text{atom}$, is very close to

the experimental value of $1.04 \pm 0.14 \mu_B/\text{atom}$.²³ This noncollinear state is followed by two degenerate collinear magnetic structures and both of them lie 170 meV higher in energy compared to the ground state.

A noncollinear centered antiprism with $5.33 \mu_B$ moment (Fig.1m) is found to be the ground state for Mn_9 cluster. This structure has very high noncollinearity, $\theta \sim 48^\circ$. We find another less noncollinear state with θ being 1.92° , which has very tiny magnetic moment is the first isomer (Fig.1). This structure lies 50 meV higher in energy compared to the ground state. The next isomer is also noncollinear in nature with comparable magnetic moment with the ground state. This structure lies 133 meV higher in energy (Fig.1o). The optimal collinear structure lies much, 181 meV, higher in energy and has a $7 \mu_B$ magnetic moment.

In our earlier work,²¹ we had found that for the Mn_{10} cluster there existed four collinear magnetic structures within a very small energy range of ~ 10 meV. There we had treated the atomic moments collinearly. In the present case, we find that a noncollinear magnetic structure (Fig.1p) with magnetic moment $5.04 \mu_B$ is lower in energy by 81 meV than the previously found optimal collinear structure. This structure is highly noncollinear with θ being 42° . All these structures, whatever collinear or noncollinear, has a pentagonal ring and can be seen as incomplete 13-atom icosahedra.

In an earlier work²¹ for the Mn_{13} cluster, we have investigated icosahedral, cuboctahedral and a hexagonal closed packed structures within the collinear atomic moment assumption and found an icosahedral structure to be the ground state, with a total magnetic moment of $3 \mu_B$. The optimal hexagonal closed packed and cuboctahedral structures were found to have higher magnetic moments, 9 and $11 \mu_B$, respectively, and they lay much higher in energy (0.89 and 1.12 eV, respectively) compared to the ground state. Here we investigate only the icosahedral structure and find a noncollinear magnetic structure (Fig.2a) with $3.15 \mu_B$ moment to be degenerate with the previously found collinear ground state. The average θ is found to be small (2.5°) for this structure. Another noncollinear structure is nearly degenerate (11 meV) to the ground state with θ being 6.8° (Fig.2b). This structure has comparable magnetic moment. Another two noncollinear structures (Fig.2c-d) are found and they lie 269 and 304 meV higher, respectively.

Within the collinear atomic moment assumption,²¹ we found two different competing icosahedral structures, 5,1,5,1,3 and 1,5,1,5,1,2 staking, for the Mn_{15} cluster. Five isomers were found within ~ 60 meV of energy. The ground state had a magnetic moment of $0.87 \mu_B/\text{atom}$, whereas the experimentally measured value is rather high, $1.66 \pm 0.02 \mu_B/\text{atom}$.^{22,23} No isomer with comparable magnetic moment was found within the collinear moment assumption.²¹ At this point it would be interesting to investigate if this large discrepancy between the experimental and theoretically predicted magnetic moment is originated from collinear assumption. However, the dis-

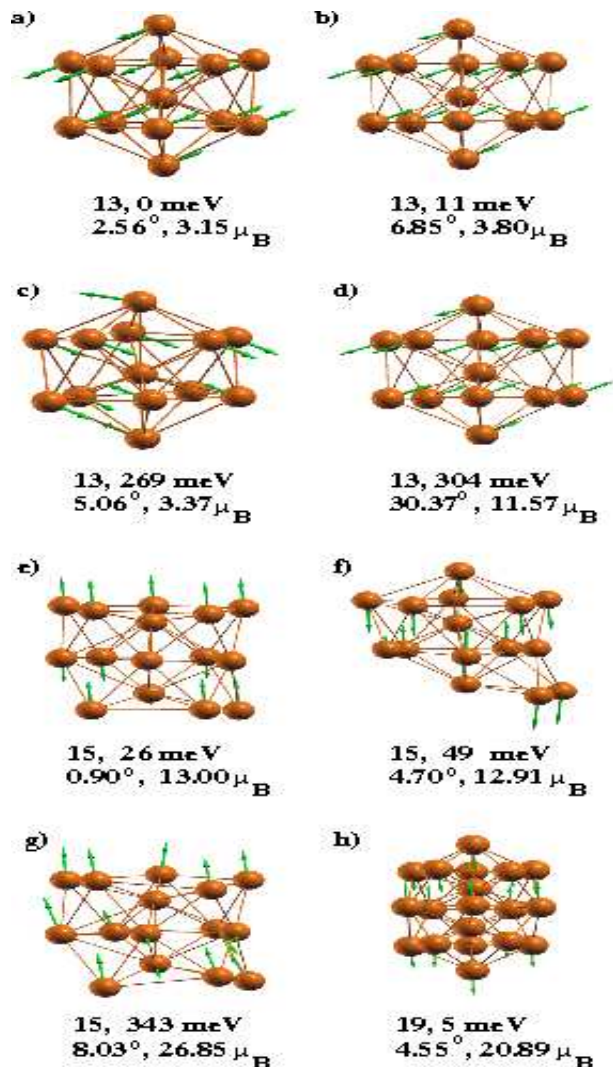


FIG. 2: (color online) Optimal noncollinear magnetic ordering for Mn_{13} , Mn_{15} and Mn_{19} .

crepancy do not improve when we relax the collinear spin assumption and treat the atomic moments noncollinearly (Table I). Two noncollinear structures (Fig.2e,f) lie very close in energy with the previously found collinear ground state. These two structures are of first and second kind of icosahedra with $\theta = 0.9^\circ$ and 4.7° , respectively. However, a structure of the first kind is found to have a magnetic moment of $1.79 \mu_B/\text{atom}$, which is close to the experimental value ($1.66 \pm 0.02 \mu_B/\text{atom}$ ^{22,23}), but this structure lies well above (343 meV) the ground state and the magnetic structure is highly noncollinear (Fig.2g).

It has experimentally been found that the magnetic moment of Mn_{19} cluster is relatively smaller than that of its neighboring clusters.^{22,23} Within the collinear moment approximation²¹, a double icosahedral structure was found to be the ground state, which had a total moment of $21 \mu_B$. This is somewhat larger than the experimentally predicted value.^{22,23} Another collinear magnetic structure with magnetic moment ($9 \mu_B$), which is

close to the experimental value lies only 75 meV higher. In the present study, which allows noncollinear arrangement of the atomic moments, we found the optimal noncollinear structure (Fig.2h) with low degree of noncollinearity to be nearly equienergetic (Table I) with the optimal collinear state.

B. As@Mn_n clusters: Effect of doping

It would now be interesting to investigate the effect of doping (for example with a single nonmagnetic atom) on the geometric and magnetic structures of Mn_n clusters. We shall dope a single nonmagnetic As-atom into an existing Mn_n cluster and shall simultaneously optimize both the geometry and magnetic ordering. The determination of the true ground state is a delicate task as the number of atoms in the cluster increases. This was true for the pure Mn_n clusters, where we found many isomers within very small energy window. The situation is equally complicated for the doped case. The Table III shows the magnetic ordering of the low lying states for As@Mn_n clusters in the size range $n=1-10$. The relaxed structures are shown in Fig.3. We had discussed²⁴ that the single nonmagnetic As doping does not alter the geometry considerably and can be derived from its pure counterpart with a moderate perturbation. However, the magnetic structure is strongly influenced by doping, which will be discussed in detail.

The AsMn dimer has much higher binding energy of 1.12 eV/atom and much shorter bond length (2.21 Å) than those of Mn₂ dimer: 0.52 eV/atom and 2.58 Å, respectively.²¹ We have repeated our calculations of AsMn dimer including the Mn 3*p* as valence electrons and obtained an optimized bond length of 2.22 Å and binding energy of 1.08 eV/atom, with the same total magnetic moment, which confirms that the inner Mn-3*p* electrons contributes insignificantly to the bonding.

The Mn-Mn coupling is found to be ferromagnetic (Fig.3a) for As@Mn₂ cluster, which has a total magnetic moment of 9 μ_B . The Mn-Mn distance in this collinear As@Mn₂ is same with the pure Mn₂ dimer. However, this collinear ground state is nearly degenerate with a noncollinear magnetic structure (Fig.3b). Another collinear structure with antiferromagnetic Mn-Mn coupling (Fig.3c) is found to be the next isomer which lies 111 meV higher than that of the ground state.

The pure Mn₃ cluster was found to be ferromagnetic with large 15 μ_B magnetic moment and is collinear in nature. The single As-atom doping reduces its magnetic moment considerably to 4 μ_B for As@Mn₃ cluster in its ground state. This structure is also collinear in nature, which is shown in Fig.3d. However, as in the pure case, there exist several isomers with different magnetic structures (Table III and Fig.3e, f). The next three isomers are all noncollinear and they lie close in energy, 5, 8 and 43 meV higher, respectively.

The optimal collinear structure with 20 μ_B magnetic

TABLE III: Type of magnetic ordering, average degree of noncollinearity⁴⁸ (θ), total magnetic moment (M_{tot}) and the relative energy difference (ΔE) for pure As@Mn_n clusters for $n=1-10$.

| Cluster | Magnetism | θ ($^\circ$) | M_{tot} (μ_B) | ΔE (meV) |
|---------------------|--------------|--------------------------|---------------------------------|---------------------|
| As@Mn | collinear | - | 4 | 0 |
| As@Mn ₂ | collinear | - | 9 | 0 |
| | noncollinear | 3.64 | 9.00 | 2 |
| As@Mn ₃ | collinear | - | 1 | 111 |
| | collinear | - | 4 | 0 |
| | noncollinear | 2.05 | 3.99 | 5 |
| As@Mn ₄ | noncollinear | 4.79 | 3.97 | 8 |
| | noncollinear | 54.46 | 0.81 | 43 |
| | collinear | - | 17 | 0 |
| As@Mn ₅ | noncollinear | 20.64 | 16.09 | 6 |
| | noncollinear | 17.63 | 16.33 | 18 |
| | collinear | - | 2 | 0 |
| As@Mn ₆ | noncollinear | 7.51 | 2.00 | 7 |
| | noncollinear | 43.73 | 9.29 | 62 |
| | noncollinear | 44.26 | 10.08 | 68 |
| As@Mn ₇ | noncollinear | 6.99 | 1.28 | 0 |
| | collinear | - | 9 | 159 |
| | noncollinear | 0.91 | 9.00 | 168 |
| As@Mn ₈ | noncollinear | 24.04 | 7.59 | 196 |
| | collinear | - | 6 | 0 |
| | noncollinear | 18.88 | 4.93 | 16 |
| As@Mn ₉ | collinear | - | 14 | 26 |
| | noncollinear | 48.77 | 6.28 | 66 |
| | noncollinear | 7.59 | 21.83 | 104 |
| As@Mn ₁₀ | noncollinear | 44.59 | 8.62 | 108 |
| | noncollinear | 0.67 | 3.00 | 0 |
| | noncollinear | 37.56 | 12.53 | 7 |
| As@Mn ₁₁ | collinear | - | 7 | 17 |
| | noncollinear | 23.45 | 10.84 | 46 |
| | noncollinear | 43.24 | 0.10 | 0 |
| As@Mn ₁₂ | collinear | - | 10 | 247 |
| | noncollinear | 8.01 | 3.88 | 353 |
| | noncollinear | 44.22 | 3.09 | 0 |
| As@Mn ₁₃ | noncollinear | 22.52 | 1.37 | 36 |
| | collinear | - | 13 | 90 |

moment was found to have 31 meV less energy than the optimal noncollinear structure for the pure tetramer. On the other hand for As@Mn₄ cluster, the optimal noncollinear structure (Fig.3h) is found to be nearly degenerate with the collinear ferromagnetic ground state (Fig.3g). The next isomer (Table III) is also noncollinear in nature and all these three structures have comparable magnetic moments.

The ground state of the As@Mn₅ cluster is found to be collinear (Fig.3i), which is nearly degenerate with the optimal noncollinear structure (Fig.3j). Both of these structures have equal magnetic moments, which are particularly small. The next two isomers are noncollinear with high noncollinearity and have comparatively large magnetic moments (Table III).

Similar to the pure Mn₆ cluster, the As@Mn₆ is found

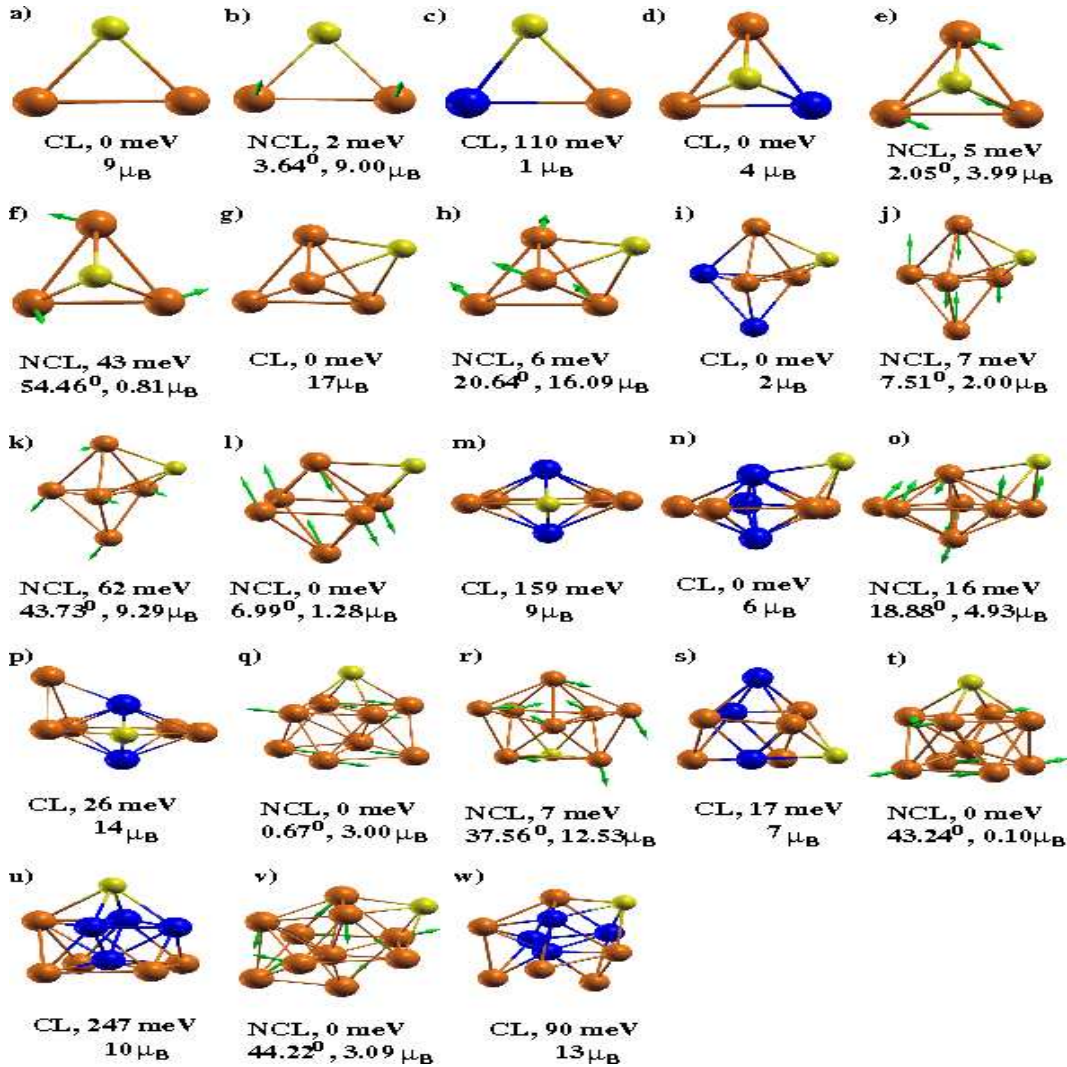


FIG. 3: (color online) The ground state and closely lying isomers of As@Mn_n clusters. The first line indicates the nature of magnetic ordering (collinear (CL) or noncollinear (NCL)) and the relative energy to the corresponding ground state (meV) and the second line indicates the average θ (in degree) for NCL case and the total magnetic moment (μ_B). For the collinear cases, orange(blue) refers the positive(negative) Mn moment. Yellow atom refers the As-atom for all the structures.

to be the smallest doped cluster, which show noncollinear magnetism (Fig.3l) in its ground state. This noncollinear structure lies 159 meV lower than the next isomer, which is collinear (Fig.3m). The noncollinear ground state has small magnetic moment ($1.28 \mu_B$) compared to the optimal collinear ($9 \mu_B$) state. The noncollinear ground state has a As-capped Mn-octahedral geometry, whereas the next (collinear) isomer is a pentagonal bi-pyramid where the As-atom sits in the pentagonal ring. Another noncollinear structure lies 196 meV higher which has large noncollinearity (24.04°) and comparable magnetic moment with the collinear structure (see Table III).

The ground state of the As@Mn_7 cluster is collinear (Fig.3n) with a total magnetic moment of $6 \mu_B$. The next isomer is noncollinear in nature with $4.94 \mu_B$ magnetic moment (Fig.3o), which lies slightly higher (16 meV) in energy. However, for pure Mn_7 cluster, the energy differ-

ence between the collinear ground state and the optimal noncollinear state is large, 232 meV (Table I); i.e. the single As doping reduces the energy difference between the collinear ground state and the optimal noncollinear state. Moreover, there exist several collinear and noncollinear structures (Table III), which are close in energy.

In an early work,²⁴ we found a collinear ground state with a magnetic moment of $3 \mu_B$ for As@Mn_8 cluster. However, after a more rigorous scan⁴⁹ of the potential energy surface we found few different magnetic states (Table III), which are lower in energy than the previously reported one. Among them a noncollinear state with very low noncollinearity (Fig.3q) is found to be the ground state. The next isomer is also noncollinear (Fig.3r), which is followed by a collinear state (Fig.3s) with $7 \mu_B$ magnetic moment.

The ground state of As@Mn_9 cluster is noncollinear

with high noncollinearity, 43.24° . However, the magnetic moment of this structure is nearly zero, $0.1 \mu_B$ (Fig.3t), which is much smaller than that of the pure Mn_9 cluster in its ground state. The next isomer is collinear in nature (Fig.3u) and has comparatively large magnetic moment, $10 \mu_B$. However, this collinear structure lies much higher, 249 meV, in energy.

We have found several isomers for the $As@Mn_{10}$ cluster (Table III). Among all a noncollinear magnetic structure (Fig.3v) with high noncollinearity (45.22°) is found to be the ground state. This structure has a total magnetic moment of $3.09 \mu_B$. The next isomer is also noncollinear which lies only 36 meV higher in energy. The optimal collinear structure have comparatively high magnetic moment and lies 90 meV higher (Fig.3w).

C. Binding energy

Binding energies of the optimal collinear and noncollinear magnetic structures have been shown in Fig.4 for both pure Mn_n and $As@Mn_n$ clusters. It has been understood²¹ that due to the lack of hybridization between the filled $4s$ states and the half-filled $3d$ states and due to high (2.14 eV) $4s^2 3d^5 \rightarrow 4s^1 3d^6$ promotion energy, Mn atoms do not bind strongly when they form clusters or crystals. This is manifested through their low

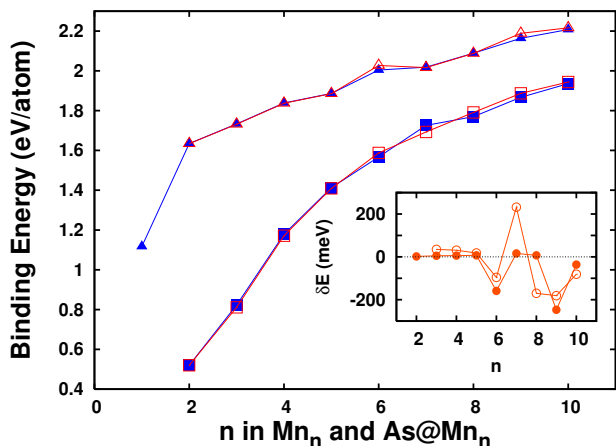


FIG. 4: (color online) Plot of binding energy for optimal collinear and noncollinear configurations as a function of Mn atoms (n) in pure Mn_n and $As@Mn_n$ clusters. Binding energy is defined as, $BE(Mn_n) = -[E(Mn_n) - n E(Mn)]/n$ for pure Mn_n clusters and $BE(As@Mn_n) = -[E(As@Mn_n) - n E(Mn) - E(As)]/(n+1)$ for $As@Mn_n$ clusters, where $E(Mn_n)$ and $E(As@Mn_n)$ are the total energies of pure Mn_n and $As@Mn_n$ clusters, respectively. The \square (\blacksquare) represents the optimal noncollinear(collinear) structures for pure Mn_n clusters, whereas, Δ (\blacktriangle) represents the optimal noncollinear(collinear) structures for $As@Mn_n$ clusters. Inset shows the total energy difference between the optimal collinear (CL) and noncollinear (NCL) configurations ($\delta E = -[E_{CL}(n) - E_{NCL}(n)]$) as a function of n . The \circ (\bullet) represent Mn_n ($As@Mn_n$) clusters.

binding energy (see Fig.4), which is the lowest among all other $3d$ - transition metal clusters. This is also experimentally evidenced through recent photodissociation experiments for cationic clusters.^{50,51} However, the bonding improves considerably due to doping of single non-magnetic As-atom.²⁴ When an As-atom is attached to the pure Mn_n clusters, due to enhanced hybridization through the As- p electrons, the binding energy of the resultant $As@Mn_n$ cluster increases substantially. It is found that the energy gain in adding an As-atom to an existing pure Mn_n cluster is much larger than that of adding a Mn-atom to an existing $As@Mn_{n-1}$ cluster.²⁴ This clearly indicates that the As-atom may act as a nucleation center for Mn-atoms.

The total energy difference, δE , between the optimal collinear and noncollinear structure for a particular sized cluster is plotted in the inset of Fig.4 as a function of n for both pure and doped clusters. By definition if δE is positive(negative) the corresponding ground state is collinear(noncollinear). For both pure Mn_n and $As@Mn_n$ clusters, the collinear states are found to be lower in energy than the corresponding optimal noncollinear states up to five Mn-atoms in the cluster and in the size range $n \geq 6$ the noncollinear states start to be the ground state with the exception for $n = 7$ for Mn_n and $n = 7$ and 8 for $As@Mn_n$ clusters. However, it should be noted here that for the entire size range there exists several collinear/noncollinear isomers which are close in energy with the corresponding ground state (see Table I and III). This establishes the importance to treat the moments noncollinearly.

D. Magnetic moment

The total magnetic moment of pure Mn_n and $As@Mn_n$ clusters of the corresponding ground states and closely lying isomers are given in Table I and Table III, respectively, and plotted in Fig.5 for the ground states. Pure Mn_n clusters in the size range $n \leq 4$ have collinear ground state and the Mn-Mn coupling is ferromagnetic. These clusters have a $5 \mu_B$ /atom magnetic moment which is the Hund's rule value for isolated Mn-atom. The magnetic moment per atom decreases drastically at $n = 5$ and the magnetic ground states start to be noncollinear for $n \geq 6$. However, we have found many collinear and noncollinear isomers with varying magnetic moment which are close in energy (not shown in Fig.5, see for instance Table I). The ground state magnetic moments of pure Mn_n clusters are compared with the SG experiment in Fig.5. Calculated magnetic moments are in good agreement with the SG experiment. However, the quantitative value differ for few clusters sizes. For an example, we find a much larger magnetic moment ($2.14 \mu_B$ /atom) for Mn_6 cluster compared to the experimental value of $0.55 \mu_B$ /atom.²³ However, our predicted value agrees with previous DFT calculation.²⁵ This quantitative discrepancy between the calculated and measured magnetic moment may arise

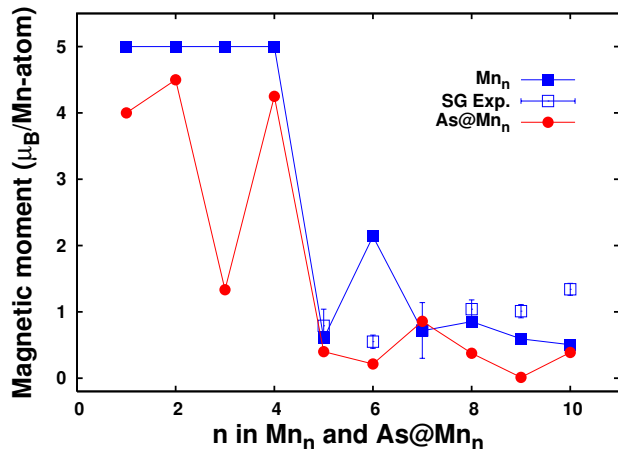


FIG. 5: (color online) Plot of magnetic moment per atom as a function of n for pure Mn_n and As@Mn_n clusters. Values only for the ground states have only been shown (see Table I and Table III for isomers). The SG experimental values for pure Mn_n clusters are shown with error bars.

from few reasons: (I) If the true ground state is missed out during the search through the potential energy surface, which is very much unlikely in the present case as we have extensively considered many different geometric and magnetic structures as initial guess. (II) In every magnetic deflection measurement the magnetic moments are calculated assuming a model (e.g. superparamagnetic, locked moment, adiabatic magnetization etc.) which might affect the outcome. (III) Due to the isomer distribution in the experimental cluster beam.

The large moment of pure Mn_n and As@Mn_n clusters arise from localized $3d$ electrons at Mn-atoms. However, the strong $p-d$ hybridization induces a small negative polarization to the As-atom. For example, this negative polarization is $0.26 \mu_B$ for AsMn dimer. However, the magnitude of this negative polarization decreases monotonically to $0.01 \mu_B$ for As@Mn_{10} cluster. Generally, the total magnetic moment of As@Mn_n cluster is lower than the corresponding pure Mn_n cluster due to $p-d$ hybridization. Similar to their pure counterparts, the Mn-Mn coupling in As@Mn_2 and As@Mn_4 is collinear ferromagnetic and the emergence of noncollinear ground state is seen at $n=6$. Moreover, it has been seen that Mn-Mn

exchange coupling in As@Mn_n clusters show anomalous behavior compared to Ruderman-Kittel-Kasuya-Yosida (RKKY) type predictions.²⁴ For collinear ground state of As@Mn_2 cluster exchange coupling oscillates between positive and negative with Mn-Mn separation (r) favoring the ferromagnetic and antiferromagnetic solutions, respectively, and dies down as $1/r^3$, which is a typical RKKY-type behavior. However on the other hand, the average exchange coupling decreases with n and has strong environment dependency, which is in contradiction with the RKKY-type prediction.

IV. SUMMARY AND CONCLUSION

This study presents a systematic investigation of electronic structure and emergence of noncollinear magnetism in pure Mn_n and As@Mn_n clusters within gradient-corrected DFT approach. No considerable structural change has been found due to noncollinear treatment of atomic moments for both pure and doped manganese clusters. Moreover, single As-doping to Mn_n clusters does not give rise any considerable structural change, but only a moderate perturbation to their pure counterpart. The pure Mn_n clusters have low binding energies, which improves substantially due to single As-doping through strong $p-d$ hybridization. The ground state of both pure Mn_n and As@Mn_n clusters for $n \leq 5$ is collinear and emergence of noncollinear ground states is seen for $n \geq 6$. However, for both kind of clusters, there exist many collinear and noncollinear isomers. Due to strong $p-d$ hybridization the magnetic moments of As@Mn_n are smaller compared to their pure counterpart. This also induces a negative polarization to the As-atom in As@Mn_n cluster. Although the results presented here are specific to the Mn_n and As@Mn_n clusters, they also contain more general picture: noncollinear magnetic ordering is possible in small magnetic clusters.

Acknowledgments

This work has been done under the Indian Department of Science and Technology Grant No. SR/S2/CAMP-25/2003.

* Corresponding author

Electronic address: mukulkab@mit.edu

¹ R. Lorenz, J. Hafner, S. S. Jaswal, and D. J. Sellmyer, Phys. Rev. Lett. **74**, 3688 (1995).

² M. Liebs, K. Hummler and M. Fähnle, Phys. Rev. B **51**, 8664 (1995).

³ Y. Tsunoda, J. Phys.: Condens. Matter **1**, 10427 (1989).

⁴ O. N. Mryasov, A. I. Liechtenstein, L. M. Sandratskii and V. A. Gubanov, J. Phys.: Condens. Matter **3**, 7683 (1991).

⁵ H. Zabel, J. Phys.: Condens. Matter **11** 9303 (1999).

⁶ T. Oda, A. Pasquarello and R. Car, Phys. Rev. Lett. **80**, 3622 (1998).

⁷ O. Ivanov and V. P. Antropov, J. Appl. Phys. **85**, 4821 (1999).

⁸ D. Hobbs, G. Kresse and J. Hafner, Phys. Rev. B **62**, 11556 (2000).

⁹ C. Kohl and G. F. Bertsch, Phys. Rev. B **60**, 4205 (1999).

¹⁰ M. A. Ojeda, J. Dorantes-Dávila and G. M. Pastor, Phys. Rev. B **60**, 6121 (1999).

¹¹ R. S. Tebble and D. J. Craik, *Magnetic Materials* (Wiley,

- New York, 1969) p. 48.
- ¹² D. Hobbs, J. Hafner, and D. Spišák, *Phys. Rev. B* **68**, 14407 (2003).
 - ¹³ J. Hafner and D. Hobbs, *Phys. Rev. B* **68**, 14408 (2003).
 - ¹⁴ C.G. Shull and M.K. Wilkinson, *Rev. Mod. Phys.* **25**, 100 (1953); J.S. Kasper and B.W. Roberts, *Phys. Rev.* **101** 537 (1956); J.A. Oberteuffer, J.A. Marcus, L.H. Schwartz, and G.P. Felcher, *Phys. Lett.* **28A**, 267 (1969); N. Kunitomi, Y. Yamada, Y. Nakai, and Y. Fujii, *J. Appl. Phys.* **40**, 1265 (1969); T. Yamada, N. Kunitomi, Y. Nakai, D.E. Cox, and G. Shirane, *J. Phys. Soc. Jpn.* **28**, 615 (1970); A.C. Lawson, A.C. Larson, M.C. Aronson, S. Johnson, Z. Fisk, P.C. Canfield, J.D. Thompson, and R.B. Von Dreele, *J. Appl. Phys.* **76**, 7049 (1994).
 - ¹⁵ T. Yamada and S. Tazawa, *J. Phys. Soc. Jpn.* **28**, 609 (1970).
 - ¹⁶ H. Yamagata and K. Asayama, *J. Phys. Soc. Jpn.* **33**, 400 (1972).
 - ¹⁷ P. Bobadova-Parvanova, K. A. Jackson, S. Srinivas and M. Horoi, *Phys. Rev. A* **67**, 61202(R) (2003).
 - ¹⁸ P. Bobadova-Parvanova, K. A. Jackson, S. Srinivas and M. Horoi, *J. Chem. Phys.* **122**, 14310 (2005).
 - ¹⁹ N. O. Jones, S. N. Khanna, T. Baruah and M. R. Pederson, *Phys. Rev. B* **70**, 45416 (2004)
 - ²⁰ T. M. Briere, M. H. F. Sluiter, V. Kumar and Y. Kawazoe, *Phys. Rev. B* **66**, 64412 (2002).
 - ²¹ M. Kabir, A. Mookerjee and D. G. Kanhere, *Phys. Rev. B* **73**, 224439 (2006).
 - ²² M. B. Knickelbein, *Phys. Rev. Lett.* **86**, 5255 (2001).
 - ²³ M. B. Knickelbein, *Phys. Rev. B* **70**, 14424 (2004).
 - ²⁴ M. Kabir, D. G. Kanhere and A. Mookerjee, *Phys. Rev. B* **73**, 75210 (2006).
 - ²⁵ T. Morisato, S. N. Khanna and Y. Kawazoe, *Phys. Rev. B* **72**, 014435 (2005).
 - ²⁶ R. C. Longo, E. G. Noya, and L. J. Gallego, *Phys. Rev. B* **72**, 174409 (2005).
 - ²⁷ A. Bergman, L. Nordström, A. B. Klautau, S. Frota-Pessôa and O. Eriksson, *Phys. Rev. B* **73**, 174434 (2006).
 - ²⁸ J. M. Sullivan, G. I. Boishin, L. J. Whitman, A. T. Hanbicki, B. T. Jonker, and S. C. Erwin, *Phys. Rev. B* **68**, 235324 (2003).
 - ²⁹ M. Zajac, J. Gosk, E. Grzanka, M. Kamińska, A. Twardowski, B. Strojek, T. Szy szko, and S. Podsiadlo, *J. Appl. Phys.* **93**, 4715 (2003).
 - ³⁰ D. C. Kundaliya, S. B. Ogale, S. E. Lofland, S. Dhar, C. J. Metting, S. R. Shind e, Z. Ma, B. Varughese, K.V. Ramanujachary, L. Salamanca-Riba and T. Venkatesan, *Nature Materials* **3**, 709 (2004).
 - ³¹ P. Mahadevan and A. Zunger, *Phys. Rev. B* **68**, 75202 (2003);
 - ³² M. van Schilfgaarde and O. N. Mryasov, *Phys. Rev. B* **63**, 233205 (2001).
 - ³³ J. L. Xu, M. van Schilfgaarde and G. D. Samolyuk, *Phys. Rev. Lett.* **94**, 97201 (2005).
 - ³⁴ S. J. Potashnik, K. C. Ku, S. H. Chun, J. J. Berry, N. Samarth, and P. Schiffer, *Appl. Phys. Lett.* **79**, 1495 (2001).
 - ³⁵ S. J. Potashnik, K. C. Ku, R. Mahendiran, S. H. Chun, R. F. Wang, N. Samarth, and P. Schiffer, *Phys. Rev. B* **66**, 012408 (2002).
 - ³⁶ J. Schliemann and A. H. MacDonald, *Phys. Rev. Lett.* **88**, 137201 (2002).
 - ³⁷ J. Schliemann, *Phys. Rev. B* **67**, 045202 (2003).
 - ³⁸ G. A. Fiete, G. Zaránd, B. Jankó, P. Redliński, and C. P. Moca, *Phys. Rev. B* **71**, 115202 (2005).
 - ³⁹ U. von Barth and L. Hedin, *J. Phys. C* **5**, 1629 (1972).
 - ⁴⁰ L.M. Sandratskii and P.G. Guletskii, *J. Phys. F: Met. Phys.* **16**, L43 (1986).
 - ⁴¹ J. Kübler, K. H. Höck, and J. Sticht, *J. Appl. Phys.* **63**, 3482 (1988).
 - ⁴² J. Kübler, K.H. Höck, J. Sticht, and A.R. Williams, *J. Phys. F: Met. Phys.* **18**, 469 (1988).
 - ⁴³ G. Kresse and D. Joubert, *Phys. Rev. B* **59**, 1758 (1999).
 - ⁴⁴ J. P. Perdew, K. Burke, and M. Ernzerhof, *Phys. Rev. Lett.* **77**, 3865 (1996).
 - ⁴⁵ G. Kresse and J. Furthmuller, *Phys. Rev. B* **54**, 11169 (1996).
 - ⁴⁶ S. T. Bramwell and M. J. P. Gingras, *Science* **294**, 1495 (2001).
 - ⁴⁷ G. W. Ludwig, H. H. Woodbury, and R. O. Carlson, *J. Phys. Chem. Solids* **8**, 490 (1959).
 - ⁴⁸ Due to the negative polarization of the As-atom, the summation in the equation 3 includes the As-atom too for As@Mn_n clusters.
 - ⁴⁹ After our initial report,²⁴ we have considered several more initial structures to confirm the true ground state, for each cluster. However, we did not find any new structures with energy lower than those previously reported ground states except only for As@Mn₈ cluster.
 - ⁵⁰ A. Terasaki, S. Minemoto and T. Kondow, *J. Chem. Phys.* **117**, 7520 (2002).
 - ⁵¹ K. Tono, A. Terasaki, T. Ohta and T. Kondow, *J. Chem. Phys.* **123**, 174314 (2005).